Production of NiMn2O4 hollow spheres and CoFe$_2$O$_4$ bowl-like structures by using block copolymer stabilized polystyrene spheres as a hard template

Gökhan KOÇAK[1] ⓘ, **Vural BÜTÜN[2],*** ⓘ

[1]Department of Chemistry and Chemical Process Technologies, Vocational School of Higher Education, Adıyaman University, Adıyaman, Turkey

[2]Department of Chemistry, Faculty of Science and Letters, Eskişehir Osmangazi University, Eskişehir, Turkey

Abstract: The aim of this study is to highlight the use of polystyrene (PS) latexes stabilized with block copolymers as a hard template in the production of metal oxide hollow spheres. PS latexes produced by dispersion polymerization by stabilizing with tertiary amine methacrylate-based diblock copolymer were used as a hard template in the preparation of nickel manganese oxide (NiMn$_2$O$_4$) hollow spheres and cobalt iron oxide (CoFe$_2$O$_4$) bowl-like structures. Thanks to the diblock copolymer stabilizer with tertiary amine functional groups on the PS surface, precursor salts of CoFe$_2$O$_4$ and NiMn$_2$O$_4$ were first homogeneously deposited on the surface of PS latexes with a controlled precipitation technique. Then, metal oxide hollow spheres and bowl-like structures were produced by calcination. XRD results showed that CoFe$_2$O$_4$ and NiMn$_2$O$_4$ structures were successfully obtained after calcination. The thermogravimetric analysis results showed that the CoFe$_2$O$_4$ and NiMn$_2$O$_4$ contents of the hybrid PS spheres were in the range of 26.0–28.6 wt%. SEM images showed that the inorganic-polymer spheres fused with each other after calcination to form larger magnetic CoFe$_2$O$_4$ bowl-like structures. SEM images also indicated successful production of highly rough NiMn$_2$O$_4$ hollow spheres with nanosheets on the surface.

Key words: Block copolymer, polystyrene latex, dispersion polymerization, hollow spheres, NiMn$_2$O$_4$, CoFe$_2$O$_4$

1. Introduction

Nano- and microsized metal oxides, especially used in catalysis applications, are very popular structures in material science. Among them, inorganic hollow and bowl-like micro/nanostructures, a special class of materials, are good candidates for many applications due to their large surface area, low density and large amount of interior space compared to their solid counterparts, as well as other optical and catalytic properties [1–6]. In addition, various magnetic metal oxides such as α-/γ-Fe$_2$O$_3$, Fe$_3$O$_4$, Co$_3$O$_4$, CoFe$_2$O$_4$, NiMn$_2$O$_4$ and NiFe$_2$O$_4$ can be produced [7–10]. The magnetic nature of these materials provides them with significant advantages, such as being able to be directed in the magnetic field, as well as the reduction of repetitive use and physical losses, especially in catalysis and adsorption applications [7–9]. For practical applications, it is important to produce hollow spheres and bowl-like structures in the desired size, monodisperse size distribution, repeatable and cost-effective [1–5]. Using many different approaches, it is possible to produce uniform and repeatable hollow spheres and bowl-like structures [1–4]. Among these techniques, the use of hard templates (polymer, silica and carbon) is conceptually the simplest [1,2]. Polystyrene (PS), PS derivatives, poly(methyl methacrylate) (PMMA) and formaldehyde resins are often used as polymeric hard templates due to their easy and low cost [1,2].

Polymeric spheres have been designed using different strategies, with the necessity of having groups that enable interactions on the surface of the polymeric spheres produced, in order to accumulate inorganic compounds. One of them is the spheres produced by the emulsifier-free emulsion polymerization method, and the functionality in such structures is due to the anionic or cationic structure of the radical initiator used [11,12]. Other widely preferred method is to modify the surface of PS spheres using sulfuric acid [2,11,13]. Another polymeric hard screen approach is the production of spherical brushes by polymerization initiated from the polymer surface [14–17]. Many different techniques such as photodeposition, chemical vapor deposition, electrodeposition, controlled precipitation, hydrothermal deposition, electrostatic layer-by-layer (LbL) can be used for the coating of the surface of template materials with inorganic species [1–5]. After coating process, the hollow structures are obtained by dissolving the polymeric structure in a suitable solvent or by calcination [1–

5]. With a pioneering approach proposed by us before, it is the use of block copolymer stabilizers that provide the basis for the interaction of inorganic species with PS spheres, allowing the accumulation of inorganic species on the PS surface. In our previous studies, we reported successful production of double layer nickel oxide and manganese oxide hollow spheres with a very rough surface with nanosheets on the surface [18], nickel oxide [19] and nickel iron oxide [20] hollow spheres.

In the present study, nickel manganese oxide ($NiMn_2O_4$) hollow spheres and cobalt iron oxide ($CoFe_2O_4$) bowl-like structures were produced by using block copolymer stabilized PS latexes as a hard template. The PS spheres with various sizewere produced by using poly[2-(diisopropylamino)ethyl methacrylate]-*block*-poly[2-(dimethylamino)ethyl methacrylate] (PDPA-*b*-PDMA), poly[2-(diethylamino)ethyl methacrylate]-*block*-poly[2-(dimethylamino)ethyl methacrylate] (PDEA-*b*-PDMA) and poly[2-(dimethylamino)ethyl methacrylate]-*block*-poly[2-*N*-mopholinoethyl methacrylate] (PDMA-*b*-PMEMA) diblock copolymers as stabilizer via dispersion polymerization. Thanks to the functionality provided by the tertiary amine methacrylate containing block copolymer fringes on the PS surface, it has been homogeneously coated (or deposited) with metal oxide precursor salts (metal hydroxides) in the presence of urea with the controlled precipitation technique. Finally, both polymeric compounds were removed and metal oxides were converted to $CoFe_2O_4$ and $NiMn_2O_4$ structures by calcination process. As stated above, PS spherical latexes stabilized with block copolymer, which can be produced in a simpler and more functional way than polymeric spheres to be used for this purpose, are candidates to be a new model in the production of different types of metal oxide hollow spheres.

2. Experimental section

2.1. Materials

2-(Diisopropylamino)ethyl methacrylate (DPA, SI-AL), 2-(dimethylamino)ethyl methacrylate (DMA, SI-AL), 2-(diethylamino)ethyl methacrylate (DEA, Aldrich) and 2-*N*-mofolinoethyl methacrylate (MEMA, Polysciences Inc.) monomers were first passed through the basic alumina column (SI-AL). Then, 2,2-diphenyl-1-picrylhydrazyl (DPPH) and granular calcium hydride were added and stored at –18 °C in a freezer. The monomers were distilled under vacuum before use. 1-Methoxy-1-trimethylsiloxy-2-methyl-1-propene (MTS), which is used as the initiator of the group transfer polymerization (GTP), was distilled under vacuum at room temperature. Tetra-n-butyl ammonium bibenzoate (TBABB) as a catalyst was synthesized in accordance with the literature [21]. THF was first dried with the addition of finely chopped solid sodium pieces by stirring 3 days at room temperature. It was then refluxed under dry nitrogen in the presence of solid potassium and used as a solvent in the polymerization reaction. PDPA-*b*-PDMA, PDEA-*b*-PDMA and PDMA-*b*-PMEMA diblock copolymers were synthesized by using group transfer polymerization technique as described before [22]. *n*-Pentane (Merck) was used to remove homopolymer contaminants from the diblock copolymers before proton NMR spectroscopy measurements.

Styrene (Merck) as a monomer, 2,2'-azodiisobutyronitrile (AIBN, Across) as a radical initiator, 1-propanol (SI-AL) and methanol (SI-AL) as a solvent and a diblock copolymer as stabilizer were used in the production of PS spheres via dispersion polymerization. $Fe(NO_3)_3.9H_2O$ (Panreac), $Co(NO_3)_2.6H_2O$ (Merck), $MnCl_2$ (Merck),$Ni(NO_3)_2.6H_2O$ (Merck) were used for coating the surface of PS spheres. Urea (SI-AL) has been used in the production of spherical inorganic-polymer materials for the purpose of controlled precipitation.

2.2. Instrumentation

Molecular weight distributions (M_w/M_n) and number average molecular weights (M_n) of the polymers were measured using gel permeation chromatography (GPC) having the following parameters: An Agilent Iso Pump 1200 Series and a refractive index detector, connected to PLgel Mixed-D and Mixed-E (5 and 3 μm, respectively, 300 mm × 7.5 mm, Polymer Laboratories, Amherst, MA) columns and eluted with HPLC-grade tetrahydrofuran that was stabilized with BHT (0.5 g L^{-1}) and TEA (0.02%) at a flow rate of 1.0 mL min^{-1}. PMMA standards (ex. Polymer Labs, M_n: 1100–220000 g mol^{-1}) were used for calibration. The comonomer ratio of PDPA-*b*-PDMA, PDEA-*b*-PDMA and PDMA-*b*-PMEMA diblock copolymers were determined from proton NMR spectra (deuteron solvents) by comparing related peaks of both blocks. The hydrodynamic diameters (R_h) and polydispersity index values (PDI or μ_2/G^2) of PS spheres were determined by dynamic light scattering (DLS). DLS studies were performed using the ALV/CGS-3 compact goniometer system (Malvern, Inc, UK). This goniometer system is equipped with a 22 mW He-Ne laser at λ_0 632.8 nm, a photodiode detector operating with high quantum efficiency and an ALV/LSE-5003 multitau digital correlator electronic system. All measurements were made with 90° constant angle scattering of polymer dispersions. The data were evaluated by second order cumulative analysis. The solution temperature was kept constant at ±1 °C sensitivity with a temperature controlled water bath. The wt% ratio of metal oxide or composites of metal oxide structures were determined with thermogravimetric analysis (TGA) device (Seiko SII Extar 6000 TG/DTA). Measurements were performed at different heating rates (1–10 °C min^{-1}) and under a flowing dry air atmosphere of 2 mL min^{-1}. Protherm furnaces PAF 110/10 muffle furnace was used in the

calcination process. The morphologies of PS latexes and metal oxide hollow spheres prepared were examined by light microscope (Leica DM750), and scanning electron microscope (SEM, Zeiss Evo LS10). Powder diffraction patterns of metal oxide hollow spheres were determined by X-ray diffraction (powder-XRD, PANalytical Empyrean) analysis using Cu Kα-radiation (λ¼ 1.54 Å) with 2θ angle in the range of 1–90 at room temperature. The powder diffraction patterns were examined in the HighScore Plus software and the peak determinations were made, and the phase content of the sample was illuminated with the reference phases found by searching from the ICDD PDF4+ library.

2.3. Production of PS microspheres by dispersion polymerization

In this study, PDPA-*b*-PDMA, PDEA-*b*-PDMA [22] and PDMA-*b*-PMEMA [23] diblock copolymers, which we previously produced and characterized by GTP method, were used as stabilizers (Figure 1). The detail of the production of PDPA-*b*-PDMA diblock copolymer with GTP, which is used as a stabilizer in the synthesis of PS spheres, is given in the supporting information.

Synthesis of PS microspheres (latexes) was performed using $PDPA_{0.17}$-*b*-$PDMA_{0.83}$ diblock copolymer (1.0 g, 25500 g mol^{-1}, M_w/M_n: 1.08) stabilizer, AIBN initiator (50 mg), styrene monomer (5.0 mL), 1-butanol or H_2O/methanol (50.0 mL) under nitrogen atmosphere in oil bath at 60 °C at 1000 rpm stirring speed (Figure 2). The reaction was continued
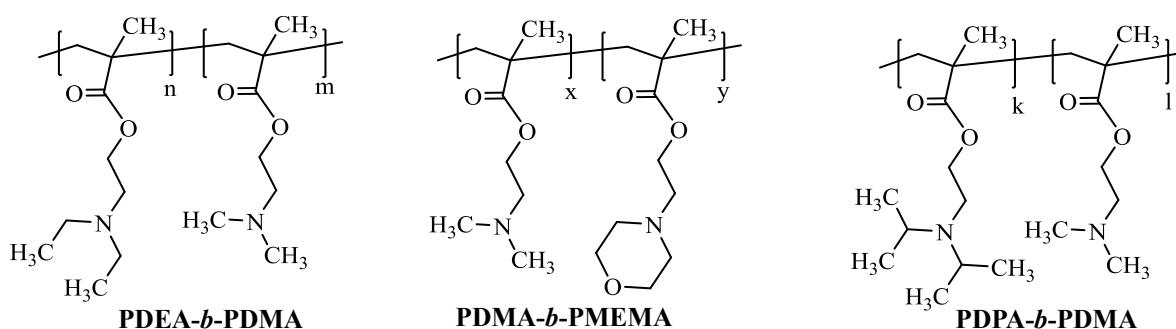

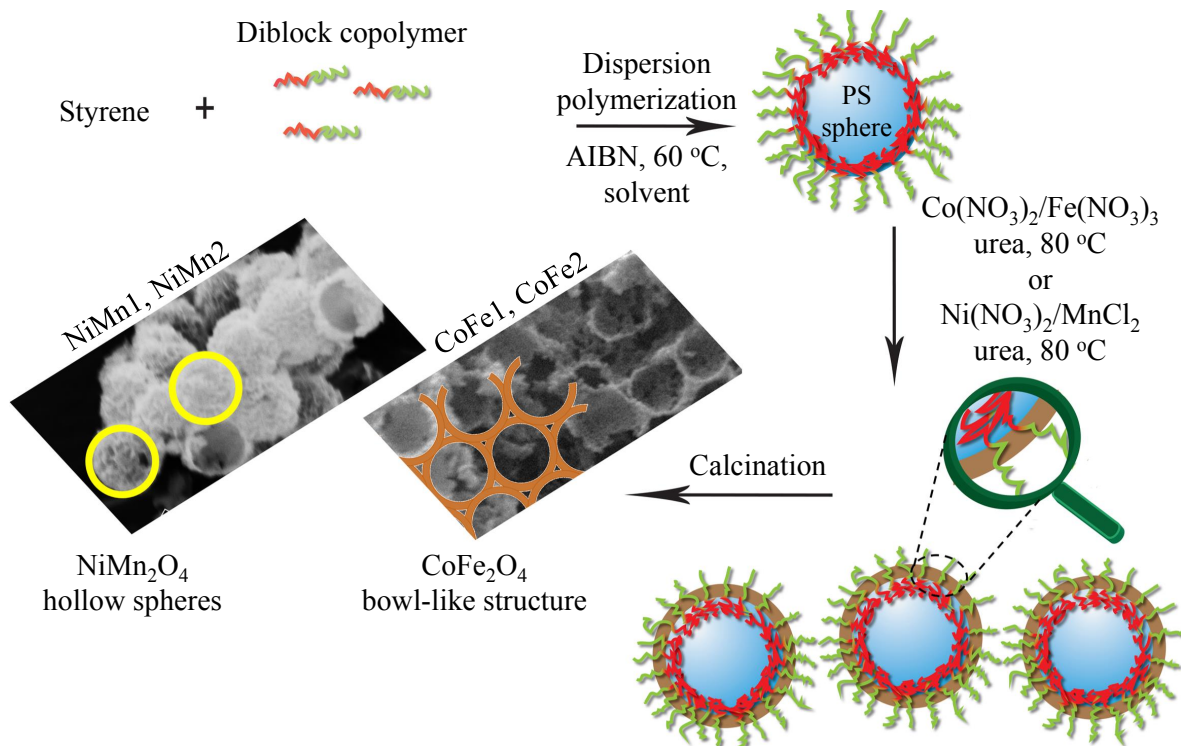**Figure 1**. Chemical structures of the diblock copolymer stabilizers.

Figure 2. Schematic representation of the production of $NiMn_2O_4$ hollow spheres and $CoFe_2O_4$ bowl-like structures using PS spheres stabilized with block copolymer.

overnight. The solution was centrifuged twice at 10000 rpm for 10 min to precipitate PS microspheres. PS spheres were dried overnight in vacuum. Experimental conditions of other produced PS spheres are given in Table 1. The spheres were characterized by DLS after centrifugation.

2.4. Preparation of metal oxide structures

Schematic representation of the production of $NiMn_2O_4$ hollow spheres and $CoFe_2O_4$ bowl-like structures using PS spheres stabilized with block copolymer are given in Figure 2. The deposition of metal hydroxides on the surface using the controlled precipitation technique in the presence of urea and then the production of both $CoFe_2O_4$ [9, 24-27] and $NiMn_2O_4$ [28, 29] structures by calcination process have been studied previously. The production of metal oxides was carried out very similar to these previous studies.

First, PS spheres (0.2 g) were dispersed in 180.0 mL of water (pH 7.0). The amounts of $Fe(NO_3)_3$ and $Co(NO_3)_2$ solutions given in Table 2 were then added and stirred for 24 h. Finally, urea was dissolved in water (20.0 mL) and added to the reaction medium and stirred at 80 °C for 24 h. Similar process was carried out using $Ni(NO_3)_2$ and $MnCl_2$ solutions, and all details are given in Table 2. The products were centrifuged three times at 5000 rpm and washed three times with distilled water. It was seen that the centrifuged solution part was completely clear, that is, all metal oxide precursor salt deposited on the PS surface in a controlled precipitation. It was observed that the PS spheres coated with both metal oxide precursor salts turned from white to brown tones over time (see Figure 3). The resulting material was dried in an oven at 100 °C overnight. The productions of all metal oxide structures are given in Table 2.

Finally, PS-inorganic hybrid spheres containing Co/Fe and Ni/Mn were calcinated at 700 °C for 1 h and at 600 °C for 2 h in air atmosphere, respectively. In these calcination processes in the furnace, both types of hybrid spheres were heated up to 300 °C and kept at this temperature for 1 h, removing most of the polymeric structure. Then it was heated from 300 °C to calcination temperatures (600 or 700 °C) with a heating rate of 1 °C/min and the calcination process was terminated by keeping at this temperature. The difference in the colors of the hybrid spheres before the calcination and the metal oxide structures formed after the calcination is given in Figure 3.

Table 1. Experimental conditions in the synthesis of the PS latexes with various size and DLS measurements (styrene 5.0 mL, 1000 rpm and at 60 °C).

Code	Stabilizer type	Stabilizer amount	AIBN	Media (50 mL)	Diameter (nm)	μ_2/G^2
PS1	[a]$PDPA_{0.17}$-b-$PDMA_{0.83}$ [b]M_n: 25500 gmol^{-1}, PDI: 1.08	1.0 g	60 mg	H_2O/MeOH (1/9)	2150	0.02
PS2	[a]$PDMA_{0.86}$-b-$PMEMA_{0.14}$ [b]M_n: 45600 g mol^{-1}, PDI: 1.13	0.6 g	45 mg	1-butanol	1050	0.08
PS3	[a]$PDEA_{0.30}$-b-$PDMA_{0.70}$ [b]M_n: 14900 g mol^{-1}, PDI: 1.06	0.6 g	45 mg	H_2O/MeOH (1/12)	1400	0.06

[a]Mole% content determined by proton NMR spectroscopy.
[b] GPC results (THF eluent, PMMA standards).

Table 2. Experimental conditions in the synthesis of the inorganic-PS hybrid spheres (in 200 mL water, at 80 °C).

Code	PS spheres (0.2 g)	Urea	$Fe(NO_3)_3$ (0.20 M)	$Co(NO_3)_2$ (0.20 M)	Residue at 650 °C (wt%)
P-CoFe1	PS1	2.0 g	4.0 mL	2.0mL	26.3
P-CoFe2	PS2	2.0 g	4.0 mL	2.0mL	28.6
Code	PS spheres (0.2 g)	Urea	$Ni(NO_3)_3$ (0.20 M)	$MnCl_2$ (0.20 M)	Residue at 650 °C (wt%)
P-NiMn1	PS3	3.0 g	2.0 mL	4.0mL	26.7
P-NiMn2	PS3	4.0 g	2.0 mL	4.0mL	26.0

The wt% ratios of metal oxides in PS-inorganic hybrid spheres were determined with by thermogravimetric analysis (TGA). TGA measurements were carried out in a dry air atmosphere (2 mL min⁻¹) and the heating program applied in the measurements is given in Figure 4. It was aimed to remove polymeric parts by keeping at approximately 300 ℃ for 60 min in TGA measurements of hybrid spheres as in the calcination process performed in the furnace. Since deviation was observed in TGA chromatograms due to intense combustion, it was planned to be kept at these temperatures for 60 min and to completely burn the polymeric part in a controlled manner. However, unexpected fluctuations were observed in TGA chromatograms, which we thought to be due to the polymer not being completely removed. The contents and morphology of the produced metal oxide structures were determined by XRD, light microscope and SEM.
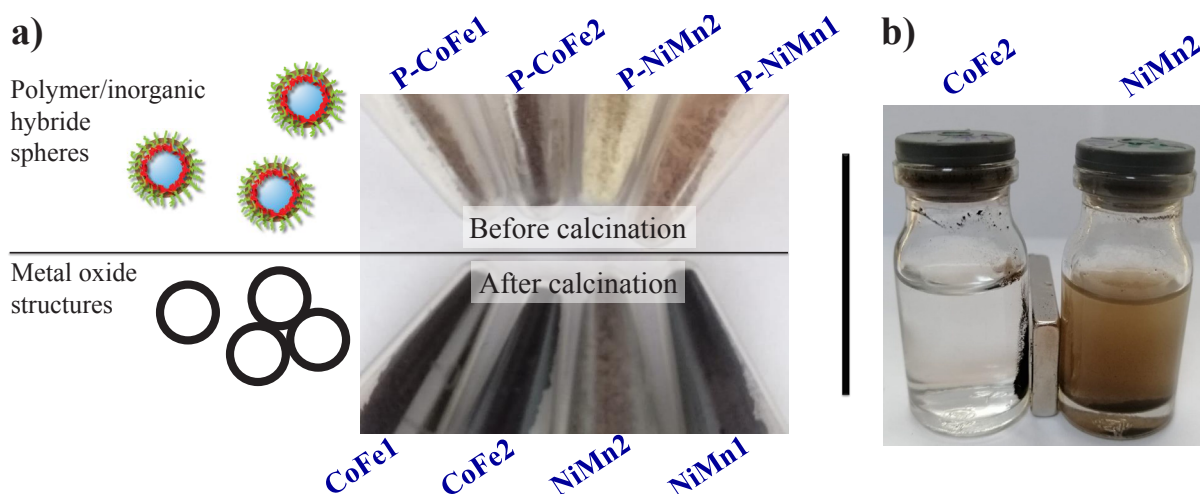

Figure 3. Digital pictures of PS-inorganic hybrid spheres (before calcination) and metal oxide structures (after calcination) (a) and the behavior of metal oxide species in a magnetic field (b).
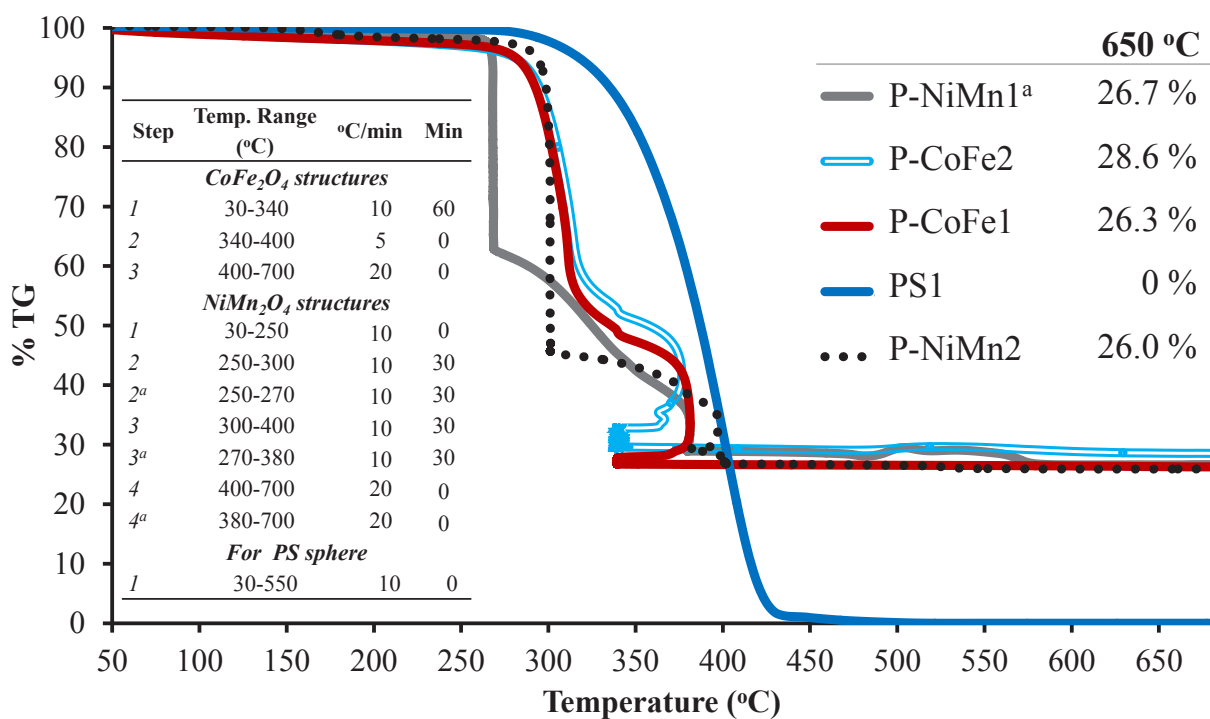

Figure 4. TGA chromatograms of PS sphere (PS1) andmetal oxide structures.

3. Results and discussion

3.1. Production of PS microspheres

The tertiary amine methacrylate based PDPA-*b*-PDMA, PDEA-*b*-PDMA and PDMA-*b*-PMEMA diblock copolymers each served as a good dispersing agent in the production of PS spheres and enabled the production of monodisperse PS spheres (Table 1). In PS latex stabilization using this block copolymer, the less soluble PDPA, PDEA or PMEMA block are adsorbed on the latex surface, while the more soluble PDMA blocks are responsible for the stabilization of latexes. The polymer chains belonging to the PDMA block are located in the form of fringes in the shell of PS spheres, just like spherical brushed polymers.

Polymeric spheres stabilized with block copolymers have been preferred by polymer scientists to produce more monodisperse or environmentally sensitive spherical particles [30–34]. The resulting spherical particles exhibit changes in swelling-shrinkage behavior or surface properties with external stimuli such as temperature and pH [30–34]. In other words, interactions are established between block copolymers and polymeric spheres used as stabilizers in emulsion and dispersion polymerization techniques. These interactions are more stronger in emulsion polymerization, but some of these block copolymers remain on the surfaces of latex after their synthesis via dispersion polymerization as well [30,34,35].

As a result of DLS studies, hydrodynamic radius (R_h) values and polydispersity index values (μ_2/G^2) of PS spheres stabilized with different block copolymers are given in Table 1. According to these results, it can be said that PS spheres are produced as monodisperse with a diameter of 1–2 μm. There are many studies showing that PS spheres can be produced in planned diameters by changing many factors such as heterogeneous polymerization technique, stabilizer type, stabilizer amount, mixing speed and solvent type [30–36]. When the previous studies are examined, if the amount of stabilizer increases or the mixing speed increases, the diameter becomes smaller. Comonomer ratios in the block copolymer have a significant effect on the diameter [23]. The type of solvent and solvent mixtures are also very effective on diameter change [36]. Since the comonomer ratios and molecular weights of the stabilizers used in the production of each PS sphere are different, it will be very difficult to compare with each other. However, it is well known that the ratios, lengths, hydrophilic/hydrophobic nature of the blocks in the stabilizer structure are decisive in ensuring that the PS diameters are at the desired size.

3.2. Preparation of metal oxide structures

In the previous section, it was mentioned that block copolymers used as stabilizers in dispersion (or emulsion) polymerization adhere to the surface [30,34,35]. The polymer fringes with this DMA unit provided a suitable environment for the absorption of metal ions. However, in this way, the metal oxide precursor salt can be deposited or adsorbed homogeneously on the structure used as a hard template. Incidentally, it is also known that PS spheres are frequently used as a hard template in the coating of polymeric cores with an inorganic layer [1,2]. PS spheres are preferred because the phenyl ring is modifiable, easy to prepare, and is a low cost polymer that is easily available commercially. In addition, poly(methyl methacrylate) and formaldehyde resin are other common polymers used for this purpose [1,2].

Together with our previous studies [18–20], it will be very useful for the reader to compare diblock copolymer stabilized PS spheres which is used as a hard template with other polymeric rigid templates in terms of functionality and production technique in this pioneering work. Inorganic species must have a surface charge (or functionality) in order to adsorb to the surface of PS spheres. This can only be achieved with stabilizing agent [30–34], anionic radical (ammonium persulfate and potassium persulfate) and cationic radical [2,2'-azobis(2-methylpropionamidine) dihydrochloride] initiators used in the emulsifier-free polymerization method [11,12], various modifications made on the phenyl ring in PS spheres [2,11,13], and spherical polymeric brush polymers, which are surface initiated polymerization products [14–17]. In addition, the fact that PS spheres have a charged surface is important in that it allows the coating of PS spheres with inorganic species with the layer-by-layer coating (LbL) technique [37]. Polymeric spheres stabilized with block copolymers contain polymer fringes around them, just like brush polymers, can be produced quite simply compared to brush polymers which are surface-initiated polymerization products that require special monomers or various modifications [14–17]. It is worth to mention that these polymeric spherical brushes are frequently used in the production of inorganic nanoparticles (NP) rather than the production of hollow spheres [14–17]. On the other hand, it is quite common to use anionic PS spheres formed by the sulfonation of the polystyrene surface with the H_2SO_4 treatment, but it can still be said that the PS spheres stabilized with the block copolymers used in this study are more functional [2,11,13]. It can be assumed that block copolymers on the surface of PS spheres provide adsorption of inorganic species to the surface and provide a completely homogeneous coating by preventing separation from the surface by forming a steric barrier during nucleation-growth [14–17].

In this study, it was thought that the mechanism of action of the diblock copolymer used to stabilize PS spheres was to establish interaction with metal ions, increase the concentration of metal ions on the PS surface with adsorption, form nuclei on the surface of the inorganic species in the basic medium, and the growth of the crystals of metal oxide precursor

salts on the PS surface thanks to the polymer fringes. The fact that tertiary amine methacrylate based polymers and many other polymers have already been discussed in many studies as metal ion adsorbents [38,39]. However, it should be kept in mind that many different types of block copolymers can be designed and used for this purpose [38,39]. It is also important that the polymer to be selected for this purpose has to have high metal ion adsorption capacity, low cost and easy availability.

Using the controlled precipitation technique as in this study, many metal oxide hollow spheres and bowl-like structures such as CuO, ZnO, SnO_2, CeO_2, MgO, α-Fe_2O_3, Cr_2O_3, In_2O_3, Co_3O_4, NiO, $CoFe_2O_4$, $NiFe_2O_4$ and other [6,40] can be produced for different applications. To summarize briefly, urea added to the reaction mixture slowly decomposes to NH_3 at 80 °C, that is, the hydroxide ion concentration in the mixture increases and metal hydroxides begin to precipitate in the PDMA fringes on the PS surface. In other words, $Fe(OH)_3/Co(OH)_2$ and $Mn(OH)_2/Ni(OH)_2$ crystals are grown in a controlled manner on the PS surface. It is then converted to $CoFe_2O_4$ and $NiMn_2O_4$ by thermal decomposition (calcination) and polymeric compounds are removed at this time [9,24–28].

According to the results of thermogravimetric analysis (TGA), it was observed that 26.0–28.6 wt% residue remains at 650 °C (Table 2). Considering that PS spheres did not leave any residue at the same temperature, almost all of the structures formed after the calcination of polymer-inorganic hybrid structures belonged to $CoFe_2O_4$ and $NiMn_2O_4$ residues (Figure 4). Of course, by adding higher proportions of precursor metal salts, these residue amounts can be further increased, and this change causing an increase in the shell thickness contributes to the hollow spheres remaining unbreakable.

Determination of the crystal phase identification of the synthesized $CoFe_2O_4$ and $NiMn_2O_4$ structures was done with XRD analysis. After 1 h of calcination at 700 °C, it was determined that CoFe1 and CoFe2 were cobalt iron oxide ($CoFe_2O_4$) with cubic and rhombohedral crystal structure, respectively. The XRD pattern of CoFe1 shows major diffraction peaks positioned at 2θ of 18.34°, 30.27°, 35.60°, 37.16°, 43.27°, 53.66°, 57.23°, 62.77° and 74.34° correspond to the planes (111), (220), (311), (222), (400), (422), (511), (440) and (533), respectively, as seen in Figure 5a. This XRD pattern is well matched with the standard ICDD: 04-006-6582. The XRD pattern reveals that the synthesized metal oxide hollow spheres are in the $CoFe_2O_4$ phase with a cubic crystal structure belonging to the space group Fd-3m. The obtained XRD pattern CoFe2 shows major diffraction peaks positioned at 2θ of 18.35°, 30.21°, 35.58°, 37.07°, 43.12°, 53.50°, 57.16°, 62.72° and 74.17° correspond to the planes (101 and 003), (110 and 104), (021 and 113), (202 and 006), (024), (300 and 214), (033 and 125), (220 and 208) and (401 and 315), respectively, as shown in Figure 5b. This XRD pattern is well matched with the standard ICDD: 04-015-9870. The obtained XRD pattern reveals that the synthesized metal oxide hollow spheres are in the $CoFe_2O_4$ phase with a rhombohedral crystal structure belonging to the space group R-3m. After 2 h of calcination at 600 °C, it was determined that nickel manganese oxide ($NiMn_2O_4$) was formed in cubic (ICDD: 04-008-6983) crystal structure. The obtained XRD pattern of NiMn1 shows major diffraction peaks positioned at 2θ of 18.35°, 30.19°, 35.58°, 37.24°, 43.3°, 53.65°, 57.18°, 62.84°, 66.01°, 71.16°, 74.25°, 75.37°, 79.44°, and 87.10° correspond to the planes (111), (220), (311), (222), (400), (422), (511), (440), (531), (620), (533), (622), (444), and (642) respectively, (see Figure 5c). This XRD pattern is well matched with the standard ICDD: 04-008-6983. The obtained XRD pattern reveals that the synthesized metal oxide hollow spheres are in the $MnNi_2O_4$ phase with a cubic crystal structure belonging to the space group Fd-3m. As seen in Figure 5, there is no other peaks related to cobalt oxide, nickel oxide, manganese oxide, iron oxide or other phases which indicate that we have pure $CoFe_2O_4$ [26] and $NiMn_2O_4$ [41].

It can be easily understood by comparing the light microscope images of PS spheres and inorganic-PS hybrid spheres that the surfaces of all PS spheres are successfully homogeneously coated with $Fe(OH)_3/Co(OH)_2$ and $Ni(OH)_2/Mn(OH)_2$ (Figure 6). Again, these images showed that no other precipitate structures were formed except for the PS surface (Figure 6). By taking SEM images of metal oxide structures, both their homogeneity and more detailed morphological structures were revealed. SEM images of the metal oxide structures taken after calcination also indicated that the PS spheres were coated homogeneously (Figure 7). From the SEM images of CoFe1 and CoFe2, it was seen that the inorganic-PS hybrid spheres fused with each other after calcination process to form larger structures (Figures 7a and 7b). Magnetic $CoFe_2O_4$ hollow bowl-like structures were obtained in the outer layer of this structure, and hollow spheres were obtained in the inner layers. The formation of these bowl-like structures resulted from the mechanical abrasion of the hollow spheres in the outer layer. The diameters of the bowl-like structures formed on the surface were, as expected, approximately 1.85 μm for CoFe1 and approximately 0.80 μm for CoFe2, in relation to the diameters of the PS spheres used. In another study where polymeric spheres were used as a rigid template and similar metal oxide type was also similar, structures with similar morphological properties were obtained, which revealed the effect of temperature [42]. Although the first structure planned to be produced is metal oxide hollow spheres, the obtained bowl-like structures can be related to the nature of the metal oxide as well as the calcination temperature and time. It is possible to produce metal oxide hollow spheres by experimenting with different calcination temperature and time [42,43]. SEM images of NiMn1 and NiMn2 samples
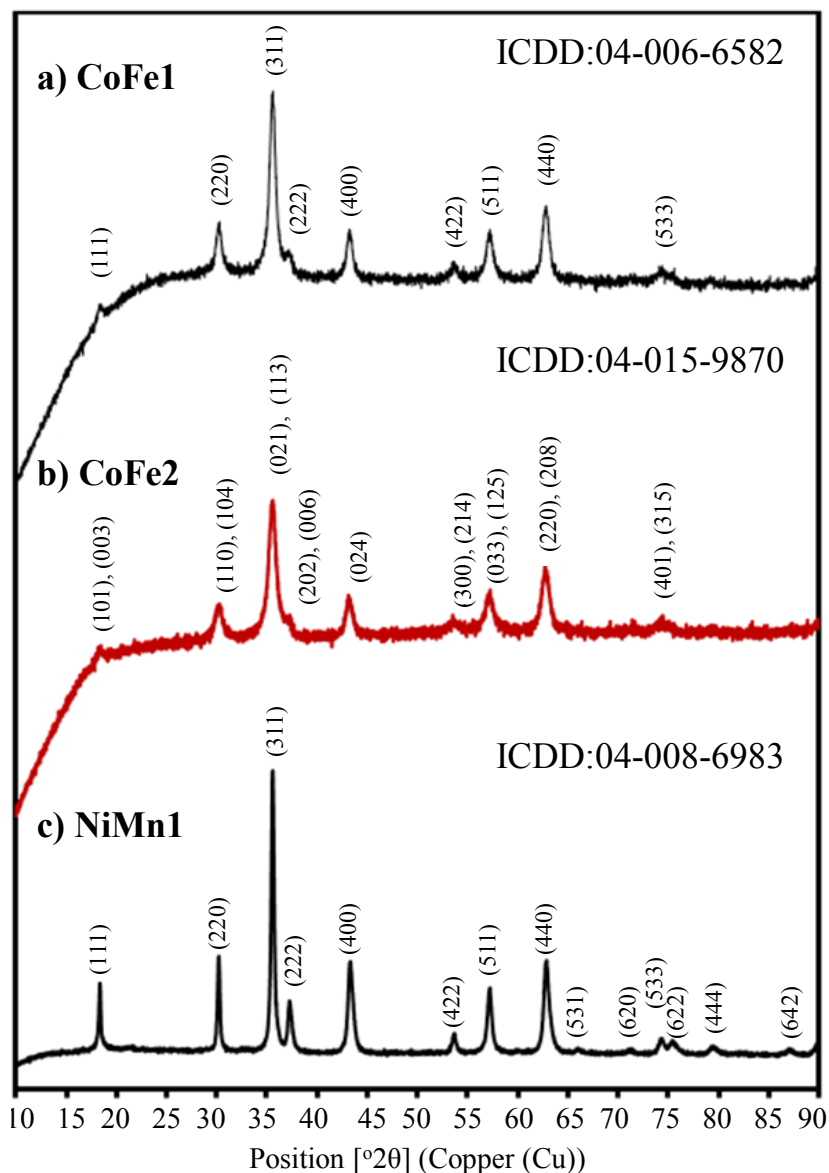
Figure 5. X-ray diffraction pattern of the prepared $CoFe_2O_4$ and $NiMn_2O_4$ structures.

showed that $NiMn_2O_4$ hollow spheres with a diameter of approximately 2.50 μm were successfully produced (Figures 7c and 7d). The reason why both have similar diameters is, of course, because they are produced using the same PS template. SEM images showed that the shell thicknesses of NiMn1 and NiMn2 hollow spheres were approximately 285 nm and 318 nm, respectively (Figure 7). The difference between NiMn1 and NiMn2 is the amount of urea and a change in the color of the resulting inorganic-PS hybrid sphere was observed (Figure 3). There were nanosheets on the surface of both $NiMn_2O_4$ hollow spheres. It has been emphasized in previous studies that the presence of nanosheets has an effect on increasing the surface area of the structure [44].

The cobalt iron oxide ($CoFe_2O_4$) is an important type of metal oxide that has applications in various fields such as sensor [45], photocatalysts [8,9], electrocatalyst [46], cancer therapy [47], batteries [25,27], magnetic optical behavior [48] and supercapacitors [49]. It is n-type semiconductor, highly stable, small optical band gaps (approximately 2.6 eV) making them active under visible light treatment [50]. The nickel manganese oxide ($NiMn_2O_4$) has been widely studied and applied in many fields such as sensor [51], negative temperature coefficient thermistors [52], photocatalysts [53], electrocatalyst [54], supercapacitors [28, 51], and batteries [55] owing to its various advantages, such as low cost, resource abundance, good stability, environmental friendliness, convenience in use and excellent electrochemical performance [56].
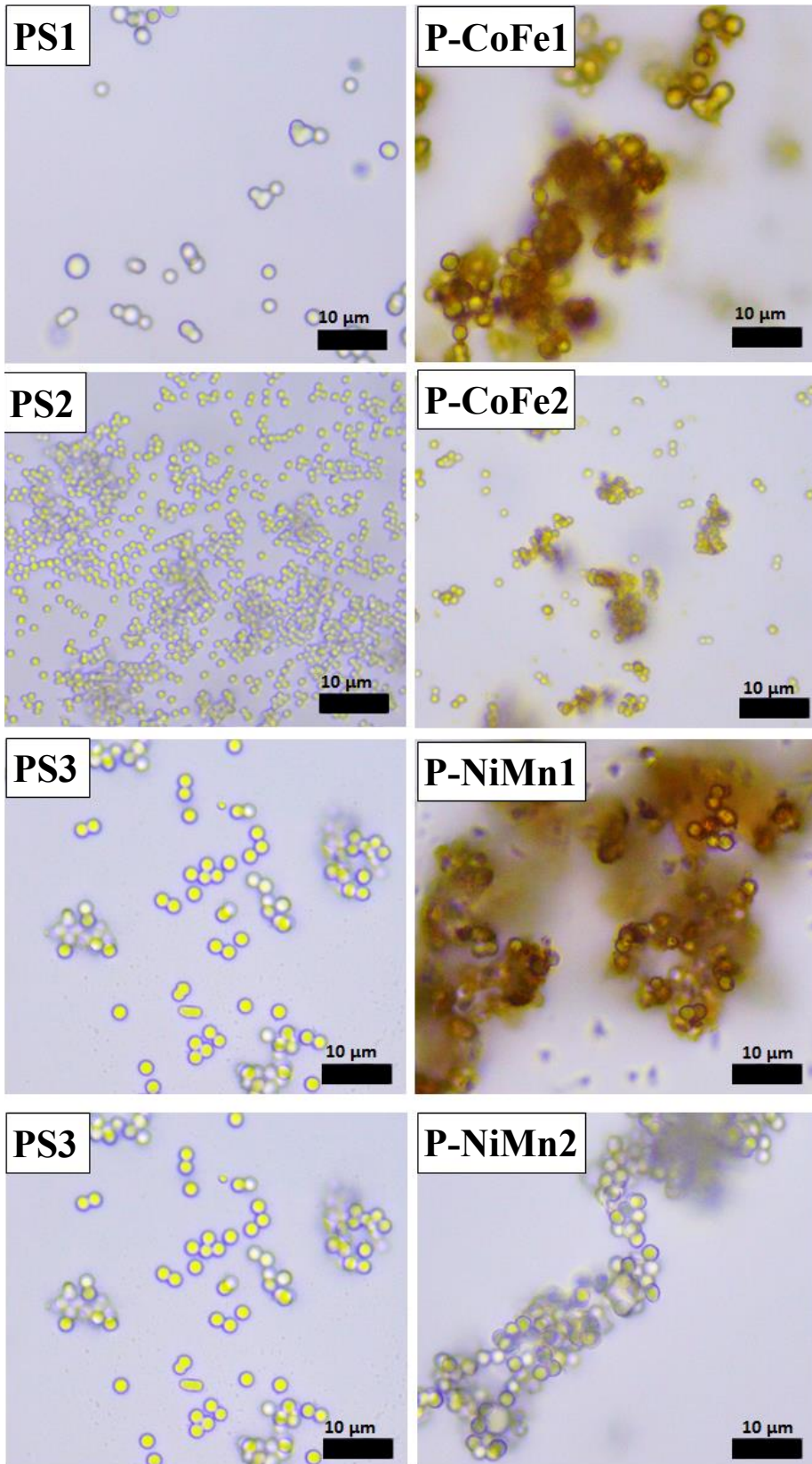
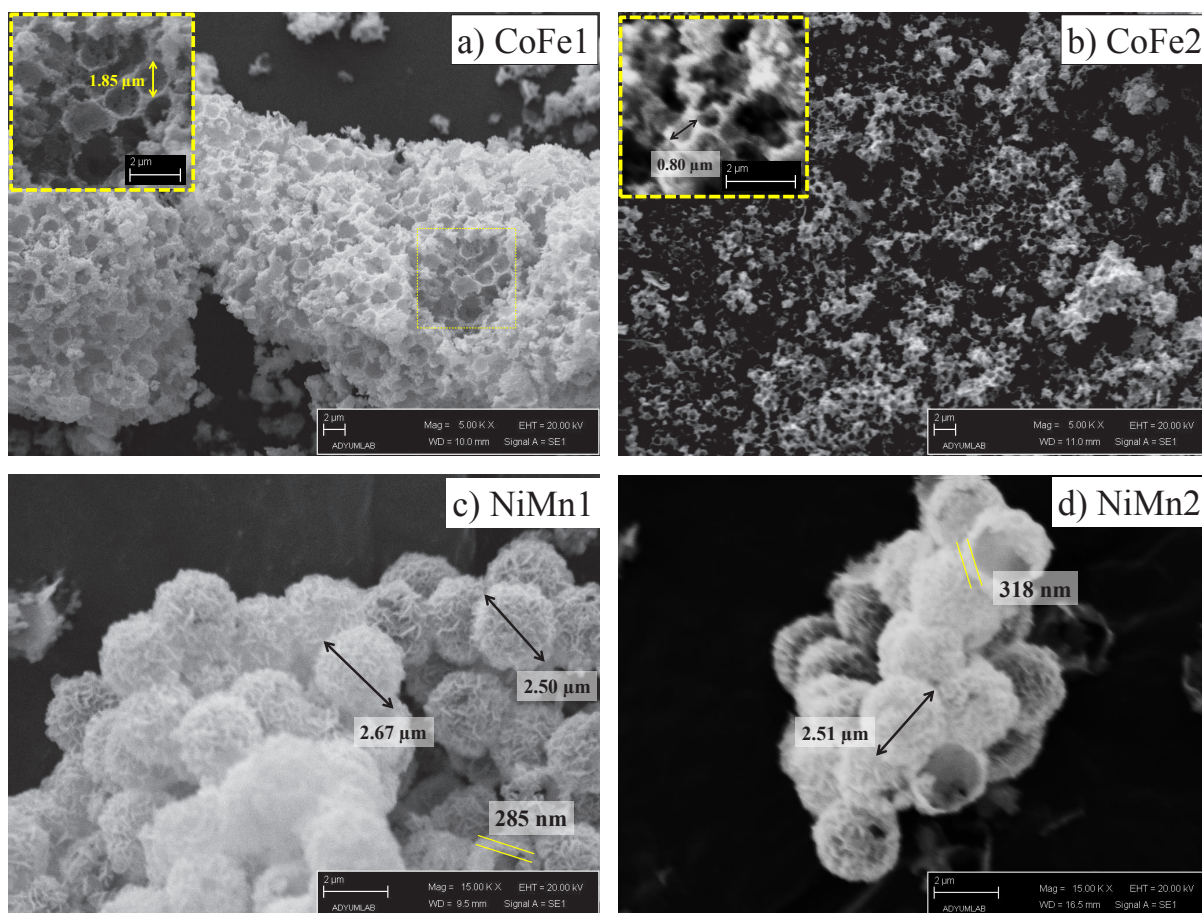**Figure 6.** Light microscope images of PS spheres and inorganic-PS hybrid spheres (before calcination).

Figure 7. SEM images of $CoFe_2O_4$ (CoFe1 and CoFe2) and $NiMn_2O_4$ (NiMn1 and NiMn2) structures produced after calcination.

The effectiveness of the materials also depends on their morphology, size and composition of the materials. In this respect, it is undoubted that reproducible and uniform metal oxide structures with varying diameters depending on the choice of polymeric sphere used as template can be used in many similar applications with the positive effect of high surface area.

4. Conclusion

The PS spheres produced in different diameters by dispersion polymerization using different diblock copolymers as stabilizers were used in the production of $NiMn_2O_4$ hollow spheres and $CoFe_2O_4$ bowl-like structures. The dimensions of these structures formed according to the diameters of the spherical spheres also changed as expected.

This study reports successful usage of spherical PS latexes stabilized with tertiary amine methacrylate based diblock copolymer as a template, which offers a new approach in terms of the use of hard templates. The surfaces of PS spheres are surrounded by a hydrated PDMA block of steric stabilizer, tertiary amine methacrylate based diblock copolymers. These stabilizers give them the ability to adsorb inorganic species at a higher capacity and stabilize the formed seeds on the surface, allowing the homogeneous metal oxide precursor salt to accumulate on the surface. Moreover, it should be noted that these PS spheres can be produced with a wide variety of block copolymers. Such hard templates have important advantages such as having more functional groups than surface modified PS spheres and being prepared with a simpler technique compared to spherical PS brushes. It is quite possible that the spheres produced in this study and other inorganic hollow spheres we continue to produce will be used in various catalysis studies in the future.

References

1.   Wang XJ, Feng J, Bai YC, Zhang Q, Yin YD. Synthesis, properties, and applications of hollow micro-/nanostructures. Chemical Reviews 2016; 116 (18): 10983-11060. doi: 10.1021/acs.chemrev.5b00731

2. HuJ, Chen M, Fang XS, Wu LW. Fabrication and application of inorganic hollow spheres. Chemical Society Reviews 2011; 40 (11): 5472-5491. doi: 10.1039/c1cs15103g

3. Liang J, Kou HR, Ding SJ. Complex hollow bowl-like nanostructures: synthesis, application, and perspective. Advanced Functional Materials 2021; 31 (10). ARTN 2007801, doi: 10.1002/adfm.202007801

4. Yang SK, Lei Y. Recent progress on surface pattern fabrications based on monolayer colloidal crystal templates and related applications. Nanoscale 2011; 3 (7): 2768-2782. doi: 10.1039/c1nr10296f

5. Ai B, Mohwald H, Wang DY,Zhang G. Advanced colloidal lithography beyond surface patterning. Advanced Materials Interfaces 2017; 4 (1): ARTN 1600271doi: 10.1002/admi.201600271

6. Boyjoo Y, Wang MW, Pareek VK, Liu J, Jaroniec M. Synthesis and applications of porous non-silica metal oxide submicrospheres. Chemical Society Reviews 2016; 45 (21): 6013-6047. doi: 10.1039/c6cs00060f

7. Zhang YQ, Huang ZB, Tang FQ, Ren J. Ferrite hollow spheres with tunable magnetic properties. Thin Solid Films 2006; 515 (4): 2555-2561. doi: 10.1016/j.tsf.2006.04.049

8. Zhang DF, Zhang GZ, Zhang L. Multi-shelled $FeCo_2O_4$ hollow porous microspheres/CCFs magnetic hybrid and its dual-functional catalytic performance. Chemical Engineering Journal 2017; 330: 792-803. doi: 10.1016/j.cej.2017.08.018

9. Bhuyan B, Paul B, Paul A, Dhar SS. Paederia foetida Linn. promoted synthesis of CoFe2O4 and NiFe2O4 nanostructures and their photocatalytic efficiency. Iet Nanobiotechnology 2018; 12 (3): 235-240. doi: 10.1049/iet-nbt.2017.0131

10. Elmaci G. Magnetic hollow biocomposites prepared from lycopodium clavatum pollens as efficient recyclable catalyst. Chemistryselect 2020; 5 (7): 2225-2231. doi: 10.1002/slct.201904152

11. Syouflan A, Inoue Y, Yada M, Nakashima K. Preparation of submicrometer-sized titania hollow spheres by ternplating sulfonated polystyrene latex particles. Materials Letters 2007; 61 (7): 1572-1575. doi: 10.1016/j.matlet.2006.07.081

12. Watanabe M, Aritomo H, Yamaguchi I, Shinagawa T, Tamai T et al. Selective preparation of zinc oxide nanostructures by electrodeposition on the templates of surface-functionalized polymer particles. Chemistry Letters 2007; 36 (5): 680-681. doi: 10.1246/cl.2007.680

13. Amari H, Guerrouache M, Mahouche-Chergui S, Abderrahim R, Carbonnier B. 2-Aminothiazole-functionalized triazine-modified polystyrene decorated with gold nanoparticles as composite catalyst for the reduction of 4-nitrophenol. Reactive & Functional Polymers 2017; 121: 58-66. doi: 10.1016/j.reactfunctpolym.2017.10.018

14. Zhu Y, Chen KM, Wang X, Guo XH. Spherical polyelectrolyte brushes as a nanoreactor for synthesis of ultrafine magnetic nanoparticles. Nanotechnology 2012; 23 (26): ARTN 265601. doi: 10.1088/0957-4484/23/26/265601

15. Nie G, Li G, Wang L, Zhang X. Nanocomposites of polymer brush and inorganic nanoparticles: preparation, characterization and application. Polymer Chemistry 2016; 7 (4): 753-769. doi: 10.1039/C5PY01333J

16. Lu Y, Hoffmann M, Yelamanchili RS, Terrenoire A, Schrinner M et al. Well-Defined crystalline TiO2 nanoparticles generated and immobilized on a colloidal nanoreactor. Macromolecular Chemistry and Physics 2009; 210 (5): 377-386. doi: 10.1002/macp.200800608

17. Polzer F, Holub-Krappe E, Rossner H, Erko A, Kirmse H et al. Structural analysis of colloidal MnOx composites. Colloid and Polymer Science 2013; 291 (3): 469-481. doi: 10.1007/s00396-012-2725-8

18. Kocak G. Use of block copolymer stabilized polystyrene microspheres as templates for preparation of hollow metal oxide spheres. Afyon Kocatepe University Journal of Science and Engineering 2020; 20 (3): 398-406. doi: 10.35414/akufemubid.680013

19. Kocak G. The use of block copolymer stabilized polystyrene microspheres as a template in the preparation of hollow nickel oxide spheres, In: The 32nd National Chemistry Congress; Online, Turkey; 2020. pp. 51. (in Turkish).

20. Kocak G. Use of block copolymer stabilized polystyrene microspheres as templates for preparation of magnetic hollow $NiFe_2O_4$ spheres, In: 4th International Mardin Artuklu Scientific Researches Conference; Mardin, Turkey; 2020. pp. 165-166.(in Turkish with an abstract in English).

21. Dicker IB, Cohen GM, Farnham WB, Hertler WR, Laganis ED et al. Oxyanions catalyze group-transfer polymerization to give living polymers. Macromolecules 1990; 23 (18): 4034-4041. doi: 10.1021/ma00220a002

22. Butun V, Armes SP, Billingham NC. Synthesis and aqueous solution properties of near-monodisperse tertiary amine methacrylate homopolymers and diblock copolymers. Polymer 2001; 42 (14): 5993-6008. doi: 10.1016/s0032-3861(01)00066-0.

23. Bütün V, Kaynak B, Esenoğlu E, Gül G. Synthesis and selective quaternization of tertiary amine methacrylate-containing water-soluble copolymers and their use in latex synthesis as stabilizers, In: Polymer Processing and Recycling Symposium and Exhibition;Mersin, Turkey; 2004. pp. 1-12. (in Turkish).

24. Suba V,Rathika G, Kumar ER, Saravanabhavan M. Influence of magnetic nanoparticles on surface changes in $CoFe_2O_4$/nerium oleander leaf waste activated carbon nanocomposite for water treatment. Journal of Inorganic and Organometallic Polymers and Materials 2018; 28 (5): 1706-1717. doi: 10.1007/s10904-018-0831-x

25. Narsimulu D, Padmaraj O, Srinadhu ES, Satyanarayana N. Synthesis, characterization and electrical properties of mesoporous nanocrystalline $CoFe_2O_4$ as a negative electrode material for lithium battery applications. Journal of Materials Science-Materials in Electronics 2017; 28 (22): 17208-17214. doi: 10.1007/s10854-017-7650-7

26. Li WC, Qiao XJ, Zheng QY, Zhang TL. One-step synthesis of MFe_2O_4 (M = Fe, Co) hollow spheres by template-free solvothermal method. Journal of Alloys and Compounds 2011; 509 (21): 6206-6211. doi: 10.1016/j.jallcom.2011.02.157

27. Yoon S. Facile microwave synthesis of $CoFe_2O_4$ spheres and their application as an anode for lithium-ion batteries. Journal of Applied Electrochemistry 2014; 44 (9): 1069-1074. doi: 10.1007/s10800-014-0716-9

28. Yan HL, Li T, Qiu KW, Lu Y, Cheng JB et al. Growth and electrochemical performance of porous $NiMn_2O_4$ nanosheets with high specific surface areas. Journal of Solid State Electrochemistry 2015; 19 (10): 3169-3175. doi: 10.1007/s10008-015-2946-0

29. Wang XL, Zhang JQ, Yang SB, Yan HY, Hong XD et al. Interlayer space regulating of NiMn layered double hydroxides for supercapacitors by controlling hydrothermal reaction time. Electrochimica Acta 2019; 295: 1-6. doi: 10.1016/j.electacta.2018.10.021

30. Bousquet A, Ibarboure E, Heroguez V, Papon E, Labrugere C et al. Single-step process to produce functionalized multiresponsive polymeric particles. Journal of Polymer Science Part A-Polymer Chemistry 2010; 48 (16): 3523-3533. doi: 10.1002/pola.24112

31. Reis BM, Armes SP, Fujii S, Biggs S. Characterisation of the dispersion stability of a stimulus responsive core-shell colloidal latex. Colloids and Surfaces a-Physicochemical and Engineering Aspects 2010; 353 (2-3): 210-215. doi: 10.1016/j.colsurfa.2009.11.015

32. Amalvy JI, Unali GF, Li Y, Granger-Bevan S, Armes SP et al. Synthesis of sterically stabilized polystyrene latex particles using cationic block copolymers and macromonomers and their application as stimulus-responsive particulate emulsifiers for oil-in-water emulsions. Langmuir 2004; 20 (11): 4345-4354. doi: 10.1021/la035921c

33. Munoz-Bonilla A,Van Herk AM, Heuts JPA. Adding stimuli-responsive extensions to antifouling hairy particles. Polymer Chemistry 2010; 1 (5): 624-627. doi: 10.1039/c0py00054j

34. Itoh T, Abe I, Tamamitsu T, Shimomoto H, Inoue K et al. Surface structure of stimuli-responsive polystyrene particles prepared by dispersion polymerization with a polystyrene/poly(L-lysine) block copolymer as a stabilizer. Polymer 2014; 55 (16): 3961-3969. doi: 10.1016/j.polymer.2014.06.069

35. Baines FL, Dionisio S, Billingham NC, Armes, SP. Use of block copolymer stabilizers for the dispersion polymerization of styrene in alcoholic media. Macromolecules 1996; 29 (9): 3096-3102. doi: 10.1021/ma951767s

36. Tuncel A, Kahraman R, Piskin E. Monosize polystyrene latices carrying functional-groups on their surfaces. Journal of Applied Polymer Science 1994; 51 (8): 1485-1498. doi: 10.1002/app.1994.070510816

37. Wang Y, Angelatos AS, Caruso F. Template synthesis of nanostructured materials via layer-by-layer assembly. Chemistry of Materials 2008; 20 (3): 848-858. doi: 10.1021/cm7024813

38. Rivas BL, Pereira ED, Moreno-Villoslada I. Water-soluble polymer-metal ion interactions. Progress in Polymer Science 2003; 28 (2): 173-208. doi: 10.1016/s0079-6700(02)00028-x

39. Rivas BL, Pereira E, Maureira A. Functional water-soluble polymers: polymer-metal ion removal and biocide properties. Polymer International 2009; 58 (10): 1093-1114. doi: 10.1002/pi.2632

40. Jiang J, Yang YM, Li LC. Surfactant-assisted synthesis of nanostructured $NiFe_2O_4$ via a refluxing route. Materials Letters 2008; 62 (12-13): 1973-1975. doi: 10.1016/j.matlet.2007.10.063

41. Periyasamy S, Subramanian P, Levi E, Aurbach D, Gedanken A et al. Exceptionally active and stable spinel nickel manganese oxide electrocatalysts for urea oxidation reaction. ACS Applied Materials & Interfaces 2016; 8 (19): 12176-12185. doi: 10.1021/acsami.6b02491

42. Srivastava AK, Madhavi S, White TJ, Ramanujan RV. Cobalt-ferrite nanobowl arrays: Curved magnetic nanostructures. Journal of Materials Research 2007; 22 (5): 1250-1254. doi: 10.1557/JMR.2007.0149

43. Li YY, Zhou F, Gao L, Duan GT. Co_3O_4 nanosheet-built hollow spheres containing ultrafine neck-connected grains templated by PS@Co-LDH and their ppb-level gas-sensing performance. Sensors and Actuators B-Chemical 2018; 261: 537-549. doi: 10.1016/j.snb.2018.01.162

44. Chu SS, Li H, Wang YZ, Ma Q, Li H et al. Porous NiO/ZnO flower-like heterostructures consisting of interlaced nanosheet/particle framework for enhanced photodegradation of tetracycline. Materials Letters 2019; 252: 219-222. doi: 10.1016/j.matlet.2019.05.145

45. Charan C, Shahi VK. Cobalt ferrite ($CoFe_2O_4$) nanoparticles (size: similar to 10 nm) with high surface area for selective non-enzymatic detection of uric acid with excellent sensitivity and stability. Rsc Advances 2016; 6 (64): 59457-59467. doi: 10.1039/c6ra08746a

46. Wang Y, Liu Q, Hu TJ, Zhang, LM, Deng YQ. Carbon supported MnO_2-$CoFe_2O_4$ with enhanced electrocatalytic activity for oxygen reduction and oxygen evolution. Applied Surface Science 2017; 403: 51-56. doi: 10.1016/j.apsusc.2017.01.127

47. Kharat PB, Somvanshi SB, Khirade PP, Jadhav KM. Induction heating analysis of surface-functionalized nanoscale $CoFe_2O_4$ for magnetic fluid hyperthermia toward noninvasive cancer treatment. ACS Omega 2020; 5 (36): 23378-23384. doi: 10.1021/acsomega.0c03332

48. Erdem D, Bingham NS, Heiligtag FJ, Pilet N, Warnicke P et al. $CoFe_2O_4$ and $CoFe_2O_4$-SiO_2 nanoparticle thin films with perpendicular magnetic anisotropy for magnetic and magneto-optical applications. Advanced Functional Materials 2016; 26 (12): 1954-1963. doi: 10.1002/adfm.201504538

49. Sapna, Budhiraja N, Kumar V, Singh SK. Synergistic effect in structural and supercapacitor performance of well dispersed $CoFe_2O_4$/Co_3O_4 nano-hetrostructures. Ceramics International 2018; 44 (12): 13806-13814. doi: 10.1016/j.ceramint.2018.04.224

50. Casbeer E, Sharma VK, Li XZ. Synthesis and photocatalytic activity of ferrites under visible light: A review. Separation and Purification Technology 2012; 87: 1-14. doi: 10.1016/j.seppur.2011.11.034

51. Umar A, Akhtar MS, Ameen S, Imran M, Kumar R et al. Colloidal synthesis of $NiMn_2O_4$ nanodisks decorated reduced graphene oxide for electrochemical applications. Microchemical Journal 2021; 160: ARTN 105630. doi: 10.1016/j.microc.2020.105630

52. Schubert M, Munch C, Schuurman S, Poulain V, Kita J et al. Novel method for ntc thermistor production by aerosol co-deposition and combined sintering. Sensors 2019; 19 (7): ARTN 1632. doi: 10.3390/s19071632

53. Abel MJ, Pramothkumar A, Archana V, Senthilkumar N, Jothivenkatachalam K et al. Facile synthesis of solar light active spinel nickel manganite ($NiMn_2O_4$) by co-precipitation route for photocatalytic application. Research on Chemical Intermediates 2020; 46 (7): 3509-3525. doi: 10.1007/s11164-020-04159-y

54. Qin Q, Chen LL, Wei T, Wang YM, Liu XE. Ni/NiM_2O_4 (M = Mn or Fe) supported on N-doped carbon nanotubes as trifunctional electrocatalysts for ORR, OER and HER. Catalysis Science & Technology 2019; 9 (7): 1595-1601. doi:10.1039/c8cy02504e

55. Li LJ, Yao Q, Liu JQ, Ye KB, Liu BY et al. Porous hollow superlattice $NiMn_2O_4$/$NiCo_2O_4$ mesocrystals as a highly reversible anode material for lithium-ion batteries. Frontiers in Chemistry 2018; 6:ARTN 153. doi: 10.3389/fchem.2018.00153

56. Wang ZB, Zhu ZH, Zhang CL, Xu CQ, Chen CN. Facile synthesis of reduced graphene oxide/$NiMn_2O_4$ nanorods hybrid materials for high-performance supercapacitors. Electrochimica Acta 2017; 230: 438-444. doi: 10.1016/j.electacta.2017.02.023

Supplementary material

Synthesis of PDPA-*b*-PDMA diblock copolymer with GTP

The synthesis of PDPA-*b*-PDMA diblock copolymer has been performed as follows using group transfer polymerization [1]: First, a 250 mL three-necked flask taken from the oven at 130 °C was placed on the vacuum line and heated with a heat gun and vacuumed in high vacuum. Solid tetra-*n*-butyl ammonium bibenzoate (TBABB) catalyst (approximately 100 mg) was added into the three-necked flask in the presence of dry nitrogen and vacuumed again. A total of 160 mL of tetrahydrofuran (THF) as solvent and 0.55 mL of 1-methoxy-1-trimethylsiloxy-2-methyl-1-propene (MTS) as initiator, respectively, were transferred into the three-necked flask via cannula. After the initiator was activated by stirring the solution for 15 min, DPA monomer (10 mL), as first monomer, was added to the reaction medium to obtain the first block. In the meantime, the temperature change of the reaction medium was observed with a contact thermocouple attached to the surface of the balloon, and it was determined that the temperature increased by 4 °C with the exothermic polymerization. The polymer solution was stirred for 40 min at room temperature. At the end of 40 min, 1 mL of sample was taken from the medium for GPC and proton NMR analysis and was terminated with 0.1 mL of methanol. The second monomer, DMA (23 mL), was added to the reaction medium under nitrogen atmosphere via a cannula, just as in the first monomer addition. A second exotherm was observed (10 °C). The reaction was stirred at room temperature for about 1 h and at the end of this period, polymerization was terminated by adding 1 mL of methanol to the reaction medium.

GPC and proton NMR analyzes were performed by taking 1 mL sample. The solid polymer obtained by evaporating the polymer solution in a rotary evaporator was dried in the freeze dryer. Homopolymer residues were observed as a result of GPC. The polymer was dissolved in THF and precipitated in *n*-pentane to get rid of these residues. As can be seen from the GPC chromatograms of the homopolymer and diblock copolymer, polymers with very narrow molecular weight distribution (M_w/M_n) have been obtained and there is no homopolymer residue in the diblock copolymer (Figure S1). GPC result indicated the number average molecular weight (M_n) and molecular weight distribution value of the diblock copolymer to be 25500 g mol^{-1} and 1.08, respectively.
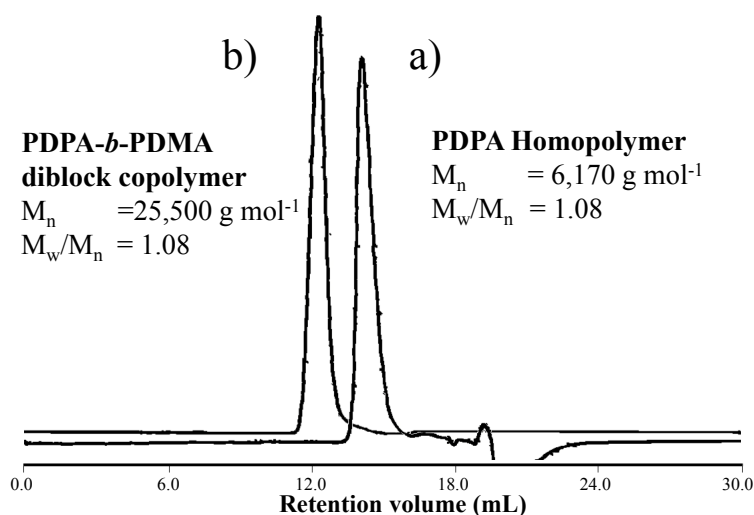

Figure S1. GPC chromatograms of PDP Ahomopolymer (a) and PDPA-*b*-PDMA diblock copolymer (b).

End group analysis was performed to determine the composition (in mol%) and polymerization degree (DP) of the PDPA-*b*-PDMA diblock copolymer. In the synthesis, first the PDPA block was produced, then the second monomer, DMA, was added and the ^{1}H NMR spectrum of the PDPA homopolymer was also taken just before addition of DMA monomer as given in Figure S2.

In order to determine comonomer ratios or mol percentages, the integral area of the isopropyl group C-H protons (**c** signal) of the PDPA at 2.94 ppm (see Figure S3) was compared with the integral area of the **a+g** signals of –C(=O)OCH$_2$- protons belonging to both PDPA and PDMA blocks in the range of 3.64–4.21 ppm (see Figure S3). The DPA and DMA contents of diblock copolymer were determined to be 16.7 mol% and 83.3 mol%, respectively. Thus the block copolymer was expressed as PDPA$_{0.17}$-*b*-PDMA$_{0.83}$. This polymer was soluble in water at room temperature. It is soluble molecularly in acidic solution but it forms micelles in neutral water or in basic conditions by PDPA block forming the micellar core.[1]
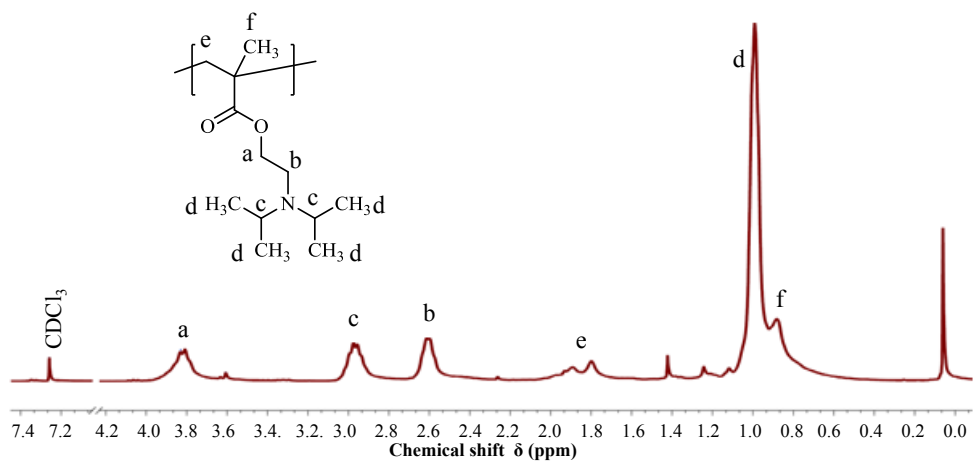
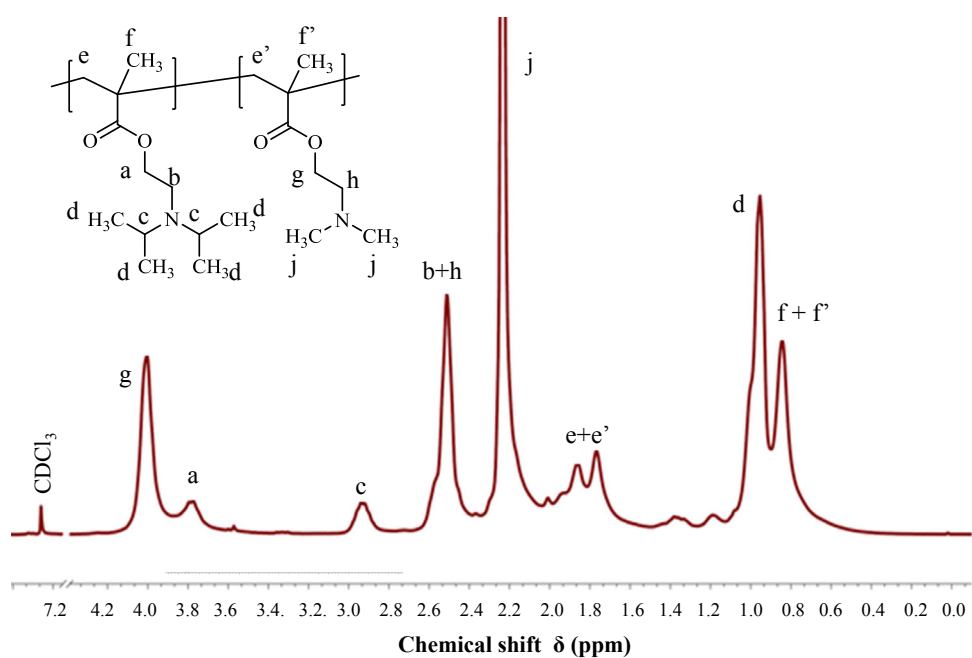**Figure S2**. ¹H NMR spectrum of PDPA homopolymer in CDCl₃.

Figure S3. ¹H NMR spectrum of PDPA-*b*-PDMA diblock copolymer in CDCl₃.

References

1.   Butun V, Armes SP, Billingham NC. Synthesis and aqueous solution properties of near-monodisperse tertiary amine methacrylate homopolymers and diblock copolymers. Polymer 2001; 42 (14): 5993-6008. doi: 10.1016/s0032-3861(01)00066-0